FULL PAPER

Interplay of Structural Flexibility and Crystal Packing in a Series of Paramagnetic Cyclopentadienyl/Dithiolene Mo and W Complexes: Evidence for Molecular Spin Ladders

Marc Fourmigué,* Benoît Domercq, Isabelle V. Jourdain, Philippe Molinié, Fabrice Guyon, and Jacques Amaudrut

In memory of Jean Rouxel

Abstract: Mixed cyclopentadienyl/dithiolene complexes of general formula [Cp$_2$M^{IV}(dithiolene)] with M = Mo, W and dmit^{2-} (2-thioxo-1,3-dithiole-4,5-dithiolate), dmid^{2-} (2-oxo-1,3-dithiole-4,5-dithiolate), and dsit^{2-} (2-thioxo-1,3-dithiole-4,5-diselenolate) as dithiolene ligand are oxidized to the six corresponding 1:1 charge-transfer salts with TCNQF$_4$ (tetrafluorotetracyanoquinodimethane), and their X-ray crystal structures are described. The structural flexibility of these complexes is evident in the large variations of the folding angle of the MQ$_2$C$_2$ plane (M = Mo or W, Q = S in dmid^{2-} and dmit^{2-}, Q = Se in dsit^{2-}) along the Q–Q hinge in the [Cp$_2$M(dithiolene)]$^{+\cdot}$ cations, and is rationalized thanks to an extended Hückel molecular orbital fragment analysis. In the solid, TCNQF$_4^{-\cdot}$ radical anions are strongly dimerized into diamagnetic [TCNQF$_4$]$_2^{2-}$ moieties, while the [Cp$_2$M(dithiolene)]$^{+\cdot}$ cations form head-to-tail dimers whose structure depends on the nature of the metal and the dithiolene ligand. These dimers organize in the solid state into various one-dimensional supramolecular structures, from quasi-regular chains to spin ladders, taking full advantage of the minute differences introduced between the different complexes (Mo vs. W, O vs. S vs. Se in the dithiolene ligands). [Cp$_2$Mo-(dmid)][TCNQF$_4$] and [Cp$_2$W(dmid)]-[TCNQF$_4$] are isostructural, the [Cp$_2$M(dmid)]$^{+\cdot}$ cations (M = Mo, W) form dimers held together by dmid/dmid overlap interactions, and they interact with each other to give spin ladders, as confirmed by the analysis of the magnetic susceptibility temperature dependence. Albeit isostructural, the Mo and W spin ladders exhibit different spin gaps, reflecting the differences between inter-molecular overlaps. Two phases were obtained from [Cp$_2$Mo(dmit)] and TCNQF$_4$, very thin needles of a 2:1 phase, [Cp$_2$Mo(dmit)]$_2$[TCNQF$_4$], and a solvent-containing 1:1 phase, shown to be [Cp$_2$Mo(dmit)][TCNQF$_4$][CH$_2$Cl$_2$]$_{0.33}$ by X-ray crystal structure determination. In the latter minor phase, [Cp$_2$Mo(dmit)]$^{+\cdot}$ forms head-to-tail dimers which interact with each other in a ladderlike motif. In [Cp$_2$W-(dmit)][TCNQF$_4$], lateral S$\cdots$S interactions lead to the formation of weak dimers, which also interact with each other in a ladder-type structure, as confirmed by analysis of the magnetic susceptibility temperature dependence. [Cp$_2$Mo(dsit)][TCNQF$_4$] and [Cp$_2$W-(dsit)][TCNQF$_4$] are isostructural; [Cp$_2$M(dsit)]$^{+\cdot}$ cations (M = Mo, W) are organized into antiferromagnetic chains in which Cp/dsit overlap interactions alternate with lateral chalcogen/chalcogen (Se, S) interactions.

Keywords: crystal engineering · dithiolene complexes · magnetic properties · molybdenum · spin ladders

Introduction

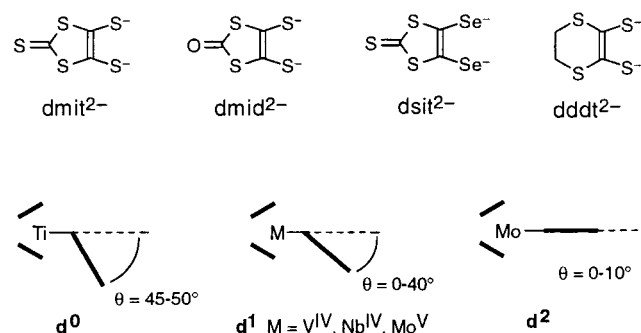The crystal engineering of molecular solids is dependent on the ability to act on the delicate balance between intermolecular interactions such as hydrogen bonds,[1, 2] π-π overlap between open-shell molecules, or both.[3] In these radical compounds, the topology of the overlap between singly occupied molecular orbitals (SOMO), typically π-type orbitals delocalized over a large part of the molecule, determines to a large extent the dimensionality of the intermolecular interactions, and therefore plays a crucial role in the competition between a localized Mott insulator state, a superconducting or metallic (pseudo-1D or 2D) state, or a 3D insulating antiferromagnetic ground state. The question of dimensionality and its manipulation are a particularly challenging task, and the specific case of low dimensionality plays a crucial role in materials science where 1D conducting chains and their associated instabilities (CDW, SDW, spin-Peierls),[4] layered organic (BEDT-TTF salts),[5, 6] and inorganic (cup-

[*] M. Fourmigué, B. Domercq, P. Molinié
Institut des Matériaux de Nantes, UMR 6502 CNRS-Université de Nantes,
2, rue de la Houssinière, BP 32229, F-44322 Nantes cedex 3 (France)
Fax: (+33) 2-40-37-39-95
E-mail: fourmigue@cnrs-imn.fr

I. V. Jourdain, F. Guyon, J. Amaudrut
Laboratoire de Chimie Organique et Organométallique,
UFR des Sciences et Techniques, F-25030 Besançon cedex (France)

rates) superconductors,[7] magnetic chains,[8, 9] and spin ladder systems[10] are of considerable present interest.

While flat, rigid radical species derived from tetrathiafulvalenes or square-planar dithiolene complexes[11, 12] are known to yield structures with recurrent 1D (Bechgaard salts) or 2D (the so-called α, β, or κ phases of ET salts) patterns—unless very large counteranions are used[13]—we expect *nonplanar, flexible, open-shell* molecules with a *delocalized spin density*, to afford novel solid-state architectures with electronic properties that reflect the distribution of intermolecular interactions, while at the same time avoiding the well-known uniform π stacking. In that respect, heteroleptic complexes of general formula [Cp$_2$M^{IV}(dithiolene)] with M = Ti, Zr, V,[14] Nb,[15] Mo, and W[16] are particularly attractive. The molybdenum complexes, which can be formally described as Mo^{IV} 18-electron d^2 species, can be reversibly oxidized[17] to the paramagnetic d^1 complexes; those bearing sulfur-rich dithiolene ligands such as [Cp$_2$Mo-(dmit)] (dmit^{2-} = 2-thioxo-1,3-dithiole-4,5-dithiolate) or [Cp$_2$Mo(dddt)] (dddt^{2-} = 5,6-dihydro-1,4-dithiine-2,3-dithiolate) proved to be appropriate candidates for the elaboration

Abstract in French: *L'oxydation de complexes mixtes cyclopentadiényl/dithiolène, de formule générale [Cp$_2$M^{IV}(dithiolène) avec M = Mo, W et comme ligand dithiolène le dmit^{2-}, le dmid^{2-} et le dsit^{2-} (dmit^{2-}: 2-thioxo-1,3-dithiole-4,5-dithiolate; dmid^{2-}: 2-oxo-1,3-dithiole-4,5-dithiolate; dsit^{2-}: 2-thioxo-1,3-dithiole-4,5-disélénolate) par le TCNQF$_4$ (tétrafluorotétracyanoquinodiméthane) conduit à la formation des six sels à transfert de charge correspondants, dont les structures cristallines sont décrites. La flexibilité structurale de ces complexes est illustrée par les différentes torsions du plan MQ$_2$C$_2$ (Q = S, Se) le long de l'axe Q–Q, déformations qu'expliquent des calculs de type Hückel étendu. Dans le solide, les anions TCNQF$_4^{-\bullet}$ s'associent en dimères diamagnétiques pendant que les radicaux cations [Cp$_2$M(dithiolène)]$^{+\bullet}$ forment des dimères tête-bêche dont l'arrangement dépend de la nature du métal et du dithiolène. Ces dimères s'organisent dans des structures étendues, chaines régulières, chaines alternées ou échelles de spin selon leur nature (Mo vs. W, O vs. S vs. Se). [Cp$_2$Mo-(dmid)][TCNQF$_4$] et [Cp$_2$W(dmid)][TCNQF$_4$] sont isostructuraux, les cations [Cp$_2$M(dmid)]$^{+\bullet}$ s'arrangent en dimères avec un recouvrement entre fragments dmid. L'analyse de la susceptibilité magnétique confirme l'organisation de ces dimères en échelle de spin, dont le gap de spin est directement corrélé aux recouvrements intra-dimères. Deux phases sont obtenues à partir de [Cp$_2$Mo(dmit)], des aiguilles très fines d'une phase 2:1, [Cp$_2$Mo(dmit)$_2$][TCNQF$_4$] et un solvate [Cp$_2$Mo(dmit)][TCNQF$_4$][CH$_2$Cl$_2$]$_{0.33}$. Une autre phase est isolée avec Cp$_2$W(dmit), qui conduit aussi à la formation d'une échelle de spin, confirmée par la dépendance en température de la susceptibilité magnétique. Enfin les sels [Cp$_2$Mo-(dsit)][TCNQF$_4$] et [Cp$_2$W(dsit)][TCNQF$_4$] sont isostructuraux, les cations [Cp$_2$M(dsit)]$^{+\bullet}$ (M = Mo, W) forment des chaines antiferromagnétiques dans lesquelles des recouvrements intermoléculaires de type Cp/dsit alternent avec des recouvrements chalcogène/chalcogène (Se, S).*

of electroactive materials with singlet–triplet antiferromagnetic interactions (Scheme 1),[18] or with an ordered three-dimensional antiferromagnetic ground state.[19] These complexes also offer a wide range of possible chemical modifica-

Scheme 1.

tions at the metal center (Mo vs. W), the cyclopentadienyl (Cp, MeCp, Cp*, ..), or the dithiolene ligands (dsit, dmid, ..). In addition to this structural variability, they also exhibit a high conformational flexibility, with a possible folding of the MS$_2$C$_2$ metallacycle along the S–S hinge. The latter is strongly dependent on the electron count and the nature of the metal and the ligands. They are thus more prone to distortion in order to accomodate different structural requirements, a rare feature which will be illustrated in this paper.

We describe a series of novel charge-transfer salts between the flexible organometallic donors [Cp$_2$M(dithiolene)] (M = Mo, W, dithiolene = dmit^{2-} (2-thioxo-1,3-dithiole-4,5-dithiolate), dmid^{2-} (2-oxo-1,3-dithiole-4,5-dithiolate), dsit^{2-} (2-thioxo-1,3-dithiole-4,5-diselenolate)) and the powerful organic π-acceptor TCNQF$_4$. Six different complexes of molybdenum and tungsten have been investigated with the aim of analyzing how comparatively minute modifications of their composition and shape influence the way they: i) organize in the solid state, ii) interact with each other, iii) the nature and iv) strength of these interactions. The structural analysis of these paramagnetic salts as well as their magnetic susceptibility temperature dependence reveal a wealth of different structural organizations based on a recurrent [{Cp$_2$M(dithiolene)$^{+\bullet}$}$_2$] radical cations dimer motif, which interacts to give an alternating spin chain or a spin ladder—a magnetic structure currently of great interest in solid-state physics.

Results and Discussion

The organometallic donor molecules and their charge-transfer salts with TCNQF$_4$: Six [Cp$_2$M(dithiolene)] complexes were prepared as previously described from the reaction of [Cp$_2$MoCl$_2$] or [Cp$_2$WCl$_2$] with the corresponding dithiolene disodium salt.[18] Three different dithiolenes were used: dmid^{2-}, dmit^{2-}, and dsit^{2-}. Dmid^{2-} and dsit^{2-} only differ from dmit^{2-} in terms of their composition. An oxygen atom is substituted for the terminal sulfur atom in dmid^{2-}, and two selenium atoms are substituted for the two coordinating sulfur

atoms in dsit^{2-}. They are known to lead to homoleptic square-planar metal (Ni, Pt, Pd) complexes whose molecular geometries[20, 21] closely resemble those of the dmit^{2-} complexes. Cyclic voltametry experiments conducted on the novel dsit^{2-} complexes, [Cp$_2$Mo(dsit)] and [Cp$_2$W(dsit)], show that they oxidize reversibly to the cationic and dicationic states at higher potentials than the corresponding dmit^{2-} complexes (Table 1). A similar shift to higher potentials upon selenium

Table 1. Cyclic voltammetry data in V vs. SCE (in CH$_3$CN, nBu$_4$NPF$_6$ 0.05 M, at 100 mV s^{-1}).

	$E^1_{1/2}$	$E^2_{1/2}$
[Cp$_2$Mo(dmit)]	0.36	0.94
[Cp$_2$Mo(dmid)]	0.31	0.96
[Cp$_2$Mo(dsit)]	0.40	0.95
[Cp$_2$W(dmit)]	0.34	0.86
[Cp$_2$W(dmid)]	0.30	0.84
[Cp$_2$W(dsit)]	0.37	0.86

substitution has been reported[22] for the oxidation of [Ni(dsit)$_2$]$^{2-}$ compared to that of [Ni(dmit)$_2$]$^{2-}$. On the other hand, the substitution of tungsten for molybdenum does not significantly modify the redox potentials of the complexes. This behavior indicates that the HOMO of those complexes has strong dithiolene character.

As shown before,[16, 18] the high oxidation potential of these complexes facilitate a reaction with an electron acceptor such as TCNQF$_4$,[23] which reduces at 0.53 V vs. SCE in CH$_3$CN.[24] Indeed, dark blue solutions, characteristic of the presence of the TCNQF$_4^{\cdot-}$ radical anion, were obtained by mixing hot solutions of the organometallic donor molecules and TCNQF$_4$. For every complex but one ([Cp$_2$Mo(dmit)], see below), slow cooling afforded black parallelepiped crystals of the 1:1 phases, [Cp$_2$Mo(dmid)][TCNQF$_4$], [Cp$_2$W(dmid)]-[TCNQF$_4$], [Cp$_2$W(dmit)][TCNQF$_4$], [Cp$_2$Mo(dsit)]-[TCNQF$_4$], and [Cp$_2$W(dsit)][TCNQF$_4$], as shown by elemental analysis and crystal structure determination. Despite the seemingly minor changes in the nature of the dithiolene ligands on substituting dmid^{2-} or dsit^{2-} for dmit^{2-}, three different crystal structures are obtained with the three different dithiolenes. Indeed, the two dmid^{2-} complexes [Cp$_2$Mo(dmid)] and [Cp$_2$W(dmid)] (Figure 1) afforded isostructural salts (triclinic, space group $P\bar{1}$) as well as the two dsit^{2-} complexes [Cp$_2$Mo(dsit)] and [Cp$_2$W(dsit)] (monoclinic, space group $P2_1/c$). A third variation was obtained with the dmit^{2-} ligand, the 1:1 salt [Cp$_2$W(dmit)][TCNQF$_4$].

In the case of [Cp$_2$Mo(dmit)], very thin needlelike crystals were obtained repeatedly, which surprisingly analyzed as [Cp$_2$Mo(dmit)]$_2$[TCNQF$_4$], that is a 2:1 salt. However, X-ray quality crystals of this stoichiometry were not obtained, but a few single crystals of a solvated 1:1 phase, [Cp$_2$Mo-(dmit)][TCNQF$_4$][CH$_2$Cl$_2$]$_{1/3}$, were isolated and their crystal structure is also reported herein. These four structures offer a unique opportunity to gain some insight in the competition between the contributions of the numerous intermolecular forces which ultimately determine the structural arrangements of the salts and, as a consequence, their magnetic properties.
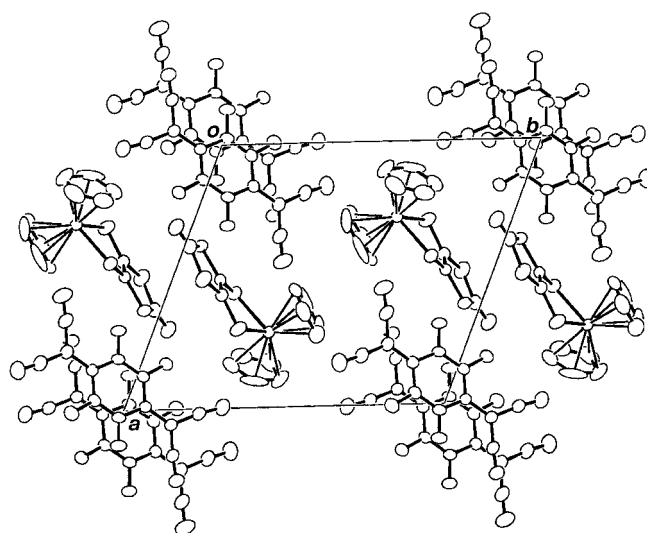

Figure 1. A view of the unit cell of [Cp$_2$Mo(dmid)][TCNQF$_4$].

The geometrical features of TCNQF$_4^{\cdot-}$ are very similar in each of the compounds (Table 2). Bond lengths are characteristic of the TCNQF$_4^{\cdot-}$ radical anion.[25] In the solid state, these radical anions form into strongly dimerized chains. Different

Table 2. Average bond lengths in TCNQF$_4^{\cdot-}$ radical anions in the salts, and corresponding values for neutral TCNQF$_4$. E.s.d. on the average values are calculated according to $\sigma = [\Sigma (d_i - d_{mean})^2/(n-1)]^{1/2}$.

	a	b	c	d	e	f
Mo/dmid	1.362(5)	1.412(8)	1.425(6)	1.418(5)	1.146(4)	1.338(4)
W/dmid	1.362(5)	1.423(9)	1.42(1)	1.42(1)	1.15(1)	1.333(8)
Mo/dmit	1.37(2)	1.40(2)	1.44(2)	1.42(4)	1.14(3)	1.35(2)
W/dmit	1.358(8)	1.420(8)	1.414(8)	1.42(1)	1.14(1)	1.341(7)
Mo/dsit	1.33(2)	1.43(2)	1.42(2)	1.43(2)	1.15(1)	1.35(2)
W/dsit	1.37(1)	1.41(2)	1.42(2)	1.43(2)	1.14(1)	1.34(2)
(TCNQF$_4^{\cdot-}$)[a]	1.360	1.420	1.429	1.435	1.140	1.349
(TCNQF$_4$)[b]	1.334	1.437	1.372	1.437	1.140	1.337

[a] In [Fe(C$_5$H$_5$)$_2$][TCNQF$_4$]: J. S. Miller, J. H. Zhang, W. M. Reiff, *Inorg. Chem.* **1987**, *26*, 600. [b] T. J. Emge, M. Maxfield, D. O. Cowan, T. J. Kistenmacher, *Mol. Cryst. Liq. Cryst.* **1981**, *65*, 161.

intra- and inter-dimer overlaps are observed in the four structural types. In the [Cp$_2$M(dmid)][TCNQF$_4$] salts (M = Mo, W), the characteristic bond-over-ring overlap with a plane-to-plane distance of 3.16 Å alternates with larger inter-dimer plane-to-plane distances at 3.30 (Mo) or 3.31 Å (W) and limited overlap, as confirmed by extended Hückel (EH) calculations of the two intra- and inter-dimer interaction energies between the LUMO of TCNQF$_4$ (Table 3). From the large intra-dimer interaction energy values, we expect the dimeric (TCNQF$_4^{\cdot-}$)$_2$ moiety to lie in a singlet state at room temperature and below. Similar conclusions can be inferred from the structural arrangements and calculated overlaps in the TCNQF$_4^{\cdot-}$ chains in [Cp$_2$Mo(dmit)][TCNQF$_4$][CH$_2$Cl$_2$]$_{1/3}$,
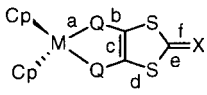
Table 3. Extended Hückel overlap interactions (double-ζ basis) in the [TCNQF$_4$·]$_2$ dimers (in eV).

	Intra-dimer	Inter-dimer
[Cp$_2$Mo(dmid)]/TCNQF$_4$	0.78	0.09
[Cp$_2$W(dmid)]/TCNQF$_4$	0.76	0.10
[Cp$_2$Mo(dmit)]/TCNQF$_4$	1.04	0.15
[Cp$_2$W(dmit)]/TCNQF$_4$	0.60	0.07
[Cp$_2$Mo(dsit)]/TCNQF$_4$	1.12	0.04
[Cp$_2$W(dsit)]/TCNQF$_4$	1.11	0.04

[Cp$_2$W(dmit)][TCNQF$_4$], and [Cp$_2$M(dsit)][TCNQF$_4$] (M = Mo, W); a sligthly weaker, laterally displaced, bond-over-ring intra-dimer overlap is observed in [Cp$_2$W(dmit)][TCNQF$_4$] and a stronger, eclipsed overlap in the other salts.

Geometrical characteristics of the [Cp$_2$M(dithiolene)] complexes in the various salts are collected in Table 4. The Mo vs. W substitution does not significantly modify the metal-

Table 4. Averaged bond lengths (a–f [Å]), angles (α–γ [°]), and the folding angle θ for the [Cp$_2$M(dithiolene)$^{+}$·] radical cations in their 1:1 TCNQF$_4$ salts. E.s.d. on the averaged values are calculated according to $\sigma = [\Sigma(d_i - d_{mean})^2/(n-1)]^{1/2}$.

Q = S, Se
α = Q—M—Q
β = M—Q—C
θ = M—Q—Q—C

Parameter	Mo/dmid	W/dmid	Mo/dmit	W/dmit	Mo/dsit	W/dsit
a	2.428(1)	2.421(2)	2.444(4)	2.426(2)	2.559(2)	2.551(1)
	2.434(1)	2.425(2)	2.448(4)	2.441(1)	2.563(2)	2.555(2)
b	1.698(5)	1.704(7)	1.684(13)	1.721(6)	1.86(1)	1.86(1)
	1.701(4)	1.722(7)	1.681(14)	1.722(6)	1.86(1)	1.89(1)
c	1.371(6)	1.37(1)	1.43(2)	1.374(8)	1.38(2)	1.33(2)
d	1.735(4)	1.740(7)	1.720(14)	1.735(6)	1.74(1)	1.77(1)
	1.732(5)	1.738(7)	1.742(13)	1.734(6)	1.73(1)	1.75(1)
e	1.766(6)	1.770(9)	1.708(13)	1.734(7)	1.72(1)	1.76(1)
	1.767(4)	1.779(9)	1.761(14)	1.738(7)	1.76(1)	1.75(1)
f	1.204(7)	1.199(9)	1.636(13)	1.635(7)	1.62(1)	1.60(1)
α	83.00(5)	83.27(7)	83.12(13)	83.18(5)	83.68(5)	83.88(5)
β	102.7(1)	101.9(2)	105.0(6)	101.5(2)	99.5(3)	98.8(4)
	102.5(2)	101.4(2)	105.2(5)	101.6(2)	99.9(4)	98.6(4)
θ	21.2(1)	26.9(1)	10.2(1)	27.56(1)	27.90(6)	32.38(1)

to-chalcogen distances, as observed in homoleptic dithiolene complexes of Mo and W.[26] Furthermore, in every complex, the MQ$_2$C$_2$ (M = Mo, W; Q = S, Se) metallacycle is folded along the Q–Q axis (Figure 2); the folding angle θ varies strongly with the nature of the metal and the dithiolene ligand, from 10.2(1)° in [Cp$_2$Mo(dmit)]$^{+}$· to 32.38(1)° in [Cp$_2$W(dsit)]$^{+}$·. Larger folding angles are observed systematically on going from Mo to W, while the order, dsit > dmid > dmit, can be established for the dithiolene ligands. This is in agreement with earlier[27] extended Hückel calculations which demonstrate that in the neutral d^2 18-electron complexes, the highest occupied Cp$_2$M fragment orbital of a$_1$ symmetry, does not interact with the highest occupied fragment orbital of the dithiolene ligand, a π-type orbital of b$_2$ symmetry. Upon oxidation, the system stabilizes by folding,
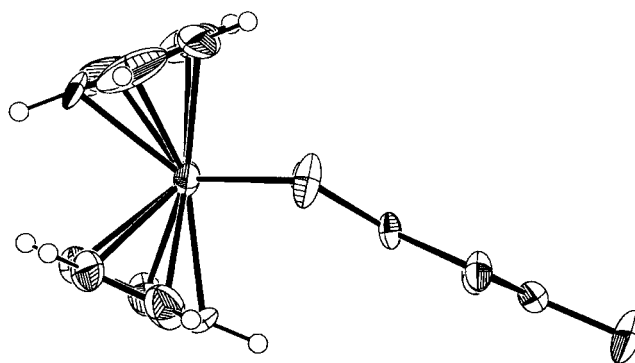
Figure 2. ORTEP lateral view of [Cp$_2$Mo(dsit)]$^{+}$·, showing the folding of the MoSe$_2$C$_2$ plane along the Se–Se axis.

this leads to a lowering of the symmetry to C_s but allows a mixing in different proportions of the two fragment orbitals (Figure 3).
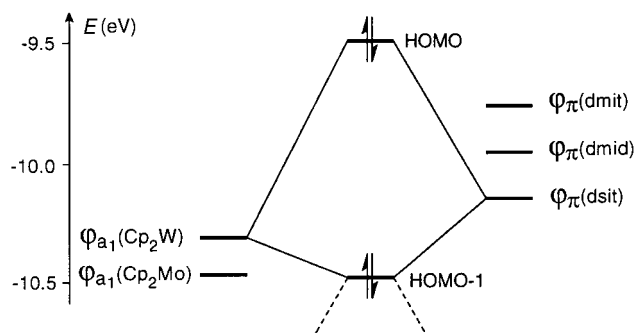
Figure 3. Extended Hückel fragment orbital interactions of the [Cp$_2$M(dithiolene)] complexes in their folded geometry.

We have already shown[14b] for d^0 complexes such as [Cp$_2$Ti(dmit)] or [Cp$_2$Ti(dddt)] that larger folding angles are a consequence of a better overlap between the fragment orbitals, which in turn relies on the relative energy levels of both fragment orbitals. The closer these energy levels are, the stronger the interaction (and θ value). Indeed, as shown in Figure 3, the fragment orbitals which are closest in energy, namely the a$_1$ metal-centered orbital of the Cp$_2$W^{2+} fragment and the π-type orbital for the dsit^{2-} fragment interact strongly, leading to the largest folding angle as observed in [Cp$_2$W(dsit)]$^{+}$·, while those fragment orbitals whose energy difference is largest, that is the Cp$_2$Mo^{2+} and dmit^{2-} moieties, generate the [Cp$_2$Mo(dmit)]$^{+}$· complex with the smallest folding angle. Accordingly, strong folding is associated with an extended mixing of the fragment orbitals and hence a lower contribution of the dithiolene to the HOMO (Figure 4). This effect will be of great importance when collections of such cation radicals will be considered in the solid state.

This amazing variety of geometries for closely related complexes illustrates two major features of solid-state chemistry of organometallic compounds, that is *structural variability* and *structural flexibility*.[28] The structural variability comes from the endless possibilities offered by the number and type of ligands, the coordination geometry, the charge of the complexes, as shown here by the chalcogen atom
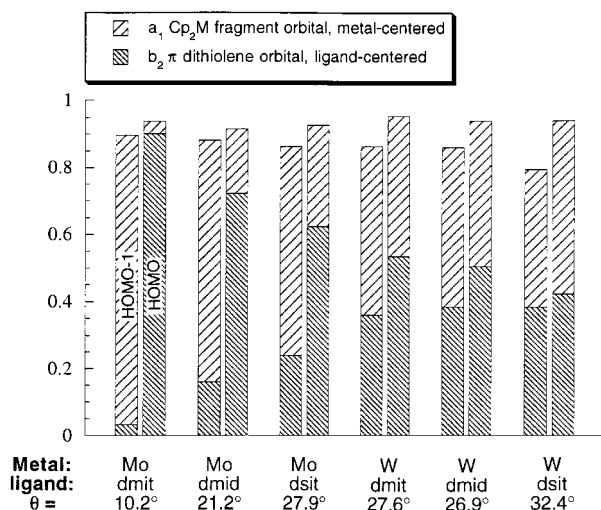
Figure 4. Contribution of the a_1 metal-centered and the b_2 ligand-centered fragment orbitals to the molecular HOMO-1 (left) and HOMO (right) for each complex, calculated in the geometry adopted in the solid state. θ is the MQ_2C_2 plane folding angle.

substitution in the series $dmid^{2-}$, $dmit^{2-}$, $dsit^{2-}$ or by the metal atom substitution in the Mo, W series. Indeed, these series offer valuable opportunities to test the effects of one modification on the whole crystal and the electronic structure of the solid. The structural flexibility is convincingly illustrated here by the broad range of folding angles θ along the S–S ($dmit^{2-}$, $dmid^{2-}$) or Se–Se ($dsit^{2-}$) hinges.

Interplay between the conformation of the dimeric $[\{Cp_2M(dithiolene)^{+\cdot}\}_2]$ units, their solid-state arrangement and their magnetic properties: For each of the four structural types encountered here, the organometallic cations systematically organize as centrosymmetrical dimers with parallel dithiolene planes; the relative orientation of the two molecules depends strongly upon the nature of the dithiolene ligand. Indeed, in the dmid complexes (Figure 5), the
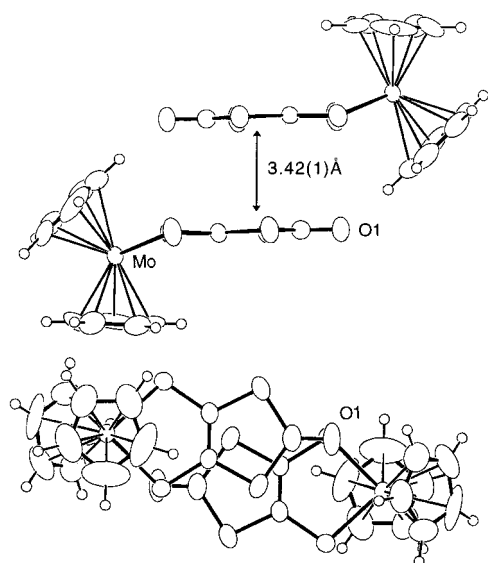

Figure 5. Side view and top view (relative to the $dmid^{2-}$ ligand) of the $[\{Cp_2Mo(dmid)^{+\cdot}\}_2]$ dimer.

dithiolene planes stack on top of each other, and display a short plane-to-plane distance which is similar in the Mo and W salts (3.42(1) (Mo) and 3.47(3) Å (W)). The two $dmid^{2-}$ ligands fit tightly into each other by positioning one sulfur atom directly above the terminal oxygen atom and an other sulfur atom in the hollow at the center of the 1,3-dithiole ring. An analogous dimer geometry is observed for $[Cp_2Mo(dmit)]^{+\cdot}$, albeit with a larger plane-to-plane distance (3.80(2) Å) which reflects the larger van der Waals radius of the outer sulfur atom of the $dmit^{2-}$ ligand. In the solid state (Figure 6), these dimeric moieties are piled up parallel to the
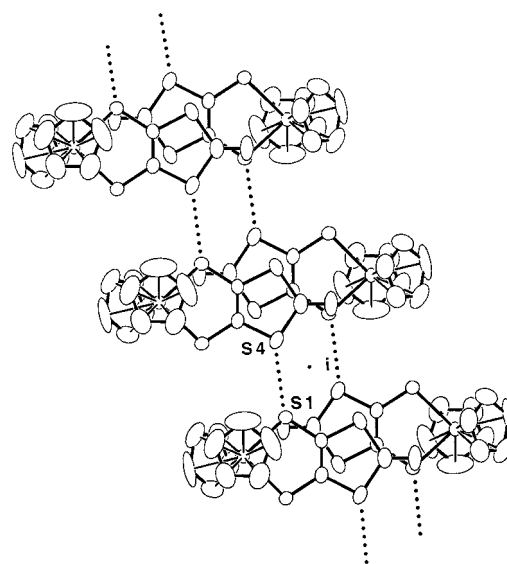

Figure 6. A view of the ladder structure adopted by the cations in the $[Cp_2M(dmid)][TCNQF_4]$ salts (M = Mo, W).

$TCNQF_4$ stacking axis, and one short lateral inter-dimer S···S contact (S1···S4 3.666(2) Å) is identified; it gives rise to an unprecedented ladder-type structure in molecular systems, the rungs are the dimeric $[\{Cp_2M(dmid)^{+\cdot}\}_2]$ units, which interact with each other along the legs parallel to the stacking axis.

Spin ladders are currently the object of theoretical and experimental investigations[29] in connection with the discovery of high-temperature superconductivity in lightly doped ladderlike antiferromagnets. However, physical realizations of spin ladders are scarce and limited to localized $S = 1/2$ copper salts such as inorganic oxides, $SrCu_2O_3$,[30] $Sr_{n-1}Cu_{n+1}O_{2n}$,[31] or $(VO)_2P_2O_7$[32], or coordination complexes such as $[Cu_2(1,4\text{-}diazacycloheptane)_2Cl_4]$.[33] Only very recently were spin ladders considered for molecular nickel dithiolene[34] or tetrathiafulvalene salts.[35, 36] This rare pattern of radical association is also found in $[Cp_2Mo(dmit)][TCNQF_4][CH_2Cl_2]_{0.33}$ in which short intermolecular S···S distances between dimers have also been identified (3.598(5) and 3.606(5) Å). As already mentioned, only a few crystals of this 1:1 phase were isolated, which precluded further magnetic susceptibility measurements.

The temperature dependence of the susceptibility of $[Cp_2Mo(dmid)][TCNQF_4]$ and $[Cp_2W(dmid)][TCNQF_4]$ is shown in Figure 7. The shape of the curves is characteristic
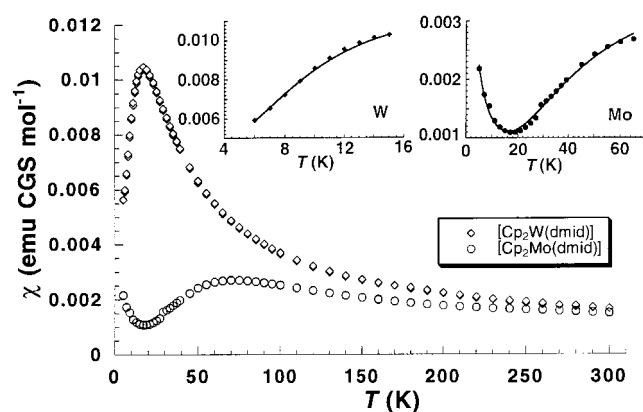
Figure 7. Temperature dependence of the magnetic susceptibility of the [Cp₂M(dmid)][TCNQF₄] salts (M = Mo, W). In insert: fits of the low-temperature data (see text).

of the presence of antiferromagnetic interactions together with a gap in the low-temperature region. They are consistent with the structural analysis which suggested the presence of ladder-type structures for both compounds (Scheme 2). Note
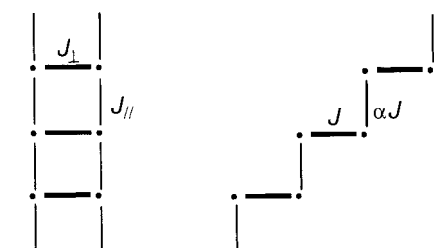
Scheme 2.

also the contribution of a Curie tail, most visible in the Mo compound. Attempts to fit the susceptibility data for both $dmid^{2-}$ compounds with a simple dimer model (Bleaney–Bower law) failed, showing that the dimers do indeed further interact with each other in the solid. Two-leg ladder systems have a finite spin gap, because a finite energy is needed to create an $S = 1$ excitation.[37] In the limit where the exchange coupling $|J_\perp|$ within the rungs is larger than the exchange coupling $|J_\parallel|$ along the chains, the ground state has a total spin of $S = 0$ because each rung is in a spin singlet. A spin of $S = 1$ excitation lies at an energy $|J_\perp|$ above the ground state, and the coupling along the chains creates a band of $S = 1$ magnetic excitations with a dispersion of about $2|J_\parallel|$. The spin gap is the minimum excitation energy as given in Equation (1).

$$\Delta_{spin} \approx |J_\perp| - |J_\parallel| + J_\parallel^2/2|J_\perp| \tag{1}$$

The magnetic susceptibility is predicted to cross over from a high-temperature Curie–Weiss form to an exponential fall-off [Eq. (2)], reflecting the finite spin gap.[38]

$$\chi \propto T^{-1/2} \exp(-\Delta_{spin}/kT) \tag{2}$$

Indeed, the low-temperature data (below the susceptibility maximum) can be fitted by Equation (2), by also taking into account the small Curie contribution. From the fits, we deduce $\Delta_{Mo} = 74$ K and $\Delta_W = 13$ K. Numerical parametrizations of a spin ladder susceptibility in the whole temperature range have been recently described by Barnes and Riera but only in the case $J_\perp/J_\parallel \leq 1.1$, which is not expected to be the case here given the strong intra-dimer interaction. We can, however, extract values of $J_\parallel$ and $J_\perp$ by considering the calculations described by Troyer, Tsunetsugu, and Würtz[41] for the situation $|J_\perp| > |J_\parallel|$. Indeed, the temperature of the susceptibility maximum $T(\chi_{max})$ is found to vary with the ratio $J_\parallel/J_\perp$, and we observed that this variation can be fitted by a quadratic function of $J_\parallel/J_\perp$ [Eq. (3)].

$$T(\chi_{max})/|J_\perp| = 0.625 - 0.01835 J_\parallel/J_\perp + 0.2532 (J_\parallel/J_\perp)^2 \tag{3}$$

By combining Equation (3) with Equation (1), we can deduce values for $J_\parallel$ and $J_\perp$ (Table 5). Note that the

Table 5. Magnetic characteristics of [Cp₂Mo(dmid)][TCNQF₄] and [Cp₂W(dmid)][TCNQF₄].

	Δ [K]	$T(\chi_{max})$ [K]	$J_\perp$ [K]	$J_\parallel$ [K]
[Cp₂Mo(dmid)][TCNQF₄]	74	70	106.8	40.7
[Cp₂W(dmid)][TCNQF₄]	13	17	23.4	15.6

antiferromagnetic interaction appears to be much stronger in the Mo compound ($J_\perp/k = -106.8$ K) than in the W compound ($J_\perp/k = -23.4$ K). Indeed, the W complex exhibits a smaller dithiolene contribution to the SOMO (see Figure 3), hence the smaller intermolecular interactions mediated through these dithiolene/dithiolene overlaps. In a Hubbard model, the exchange integral J between radicals can be related to the ratio β^2/U, where β describes the interaction energy between SOMOs and U the energy difference between the (singlet or triplet) ground state configuration, that is [Cp₂M(dmid)]⁺·[Cp₂M(dmid)]⁺· and a charge transfer configuration, that is [Cp₂M(dmid)]⁰[Cp₂M(dmid)]²⁺.[39, 40] Extended Hückel calculations of the interaction energies within a dimer afforded $\beta_{Mo} = 0.11$ eV and $\beta_W = 0.050$ eV. We deduce $(\beta_{Mo}/\beta_W)^2 = 4.8$, in very good agreement with $J_\perp(Mo)/J_\perp(W) = 4.5$. Note also that these two isostructural Mo and W salts offer a unique opportunity to possibly modify in a controlled manner the spin gap in a series of salts by crystallizing solid solutions of the two complexes, [Cp₂Mo(dmid)]ₓ[Cp₂W-(dmid)]₁₋ₓ[TCNQF₄].

[Cp₂W(dmit)⁺·][TCNQF₄⁻·] offers a second example of dimer association since the organometallic cations are no longer in a face-to-face arrangement as observed for the other structures but are laterally displaced (Figure 8), with short dmit/dmit intermolecular contacts (S3···S3 3.433(4), S3···S5 3.749(5) Å). These dimers interact with each other only through dmit/Cp interactions along the <100> TCNQF₄ stacking axis, giving rise to a ladder motif (Figure 9). Indeed, the susceptibility data (Figure 10) can not be simply depicted as the sum of a Curie tail and an isolated singlet–triplet law. From an analysis as above, we deduce a spin gap value of $\Delta_{spin}/k = 40$ K.
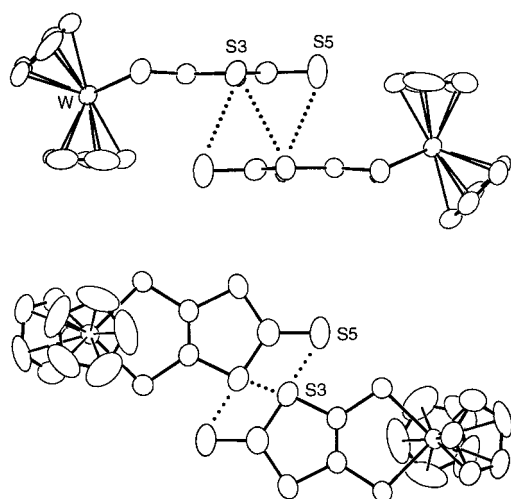
Figure 8. Side view and top view (relative to the dmit^{2-} ligand) of the [{Cp$_2$W(dmit)$^{+\cdot}$}$_2$] dimer.
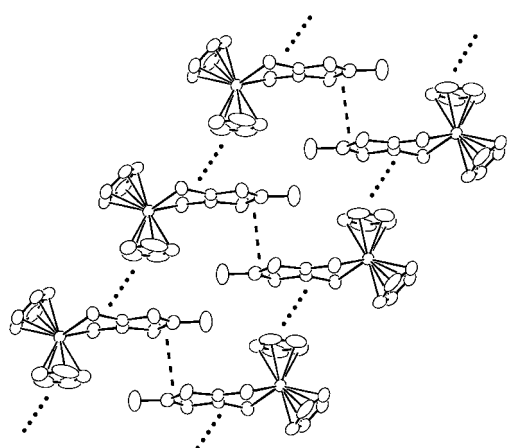
Figure 9. The ladderlike solid-state organization of the [Cp$_2$W(dmit)]$^{+\cdot}$ radical cations in [Cp$_2$W(dmit)][TCNQF$_4$]. Intra-dimer interaction: - - - -, inter-dimer interaction: ·····.

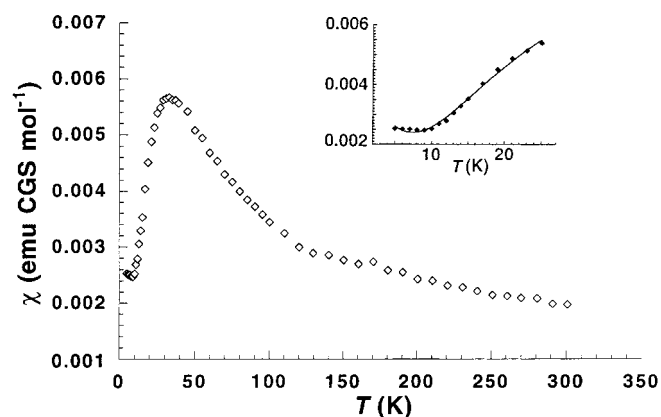Figure 10. Temperature dependence of the magnetic susceptibility of [Cp$_2$W(dmit)][TCNQF$_4$]. Insert: fit of the low-temperature data (see text).

A third, completely different interaction pattern is provided by the two isostructural Mo and W dsit^{2-} complexes. Within a dimer, the two parallel dsit planes are now 4.57 (Mo) and 4.55 Å (W) apart; the Se $\cdots$ Se distances (4.559(2) (Mo)

and 4.504(2) Å (W)) are more than twice the Se van der Waals radius (≈ 2 Å) (Figure 11). However, carbon atoms of one of the Cp rings are actually close to the sulfur atoms of the dsit

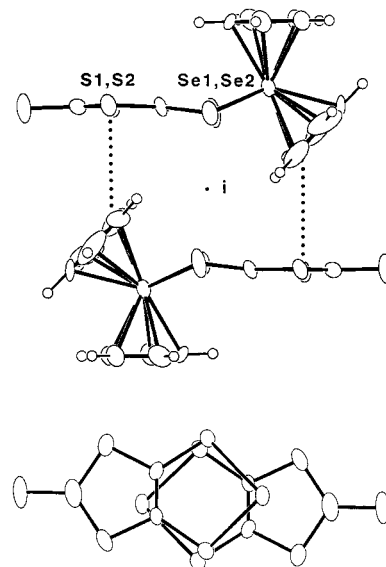Figure 11. Side view and top view (relative to the dsit^{2-} ligand) of the [{Cp$_2$Mo(dsit)$^{+\cdot}$}$_2$] dimer. The Cp rings have been omitted for clarity in the view perpendicular to the dsit plane.

moiety of the other molecule (S1$\cdots$C10 3.51(2), S2$\cdots$C9 3.62(2) Å). This intermolecular dsit/Cp interaction is expected to be sizeable since, as seen above, the large folding angle exhibited by these complexes leads to a strong contribution of the Cp$_2$M^{2+} fragment orbital to the SOMO. Indeed the corresponding intra-dimer interaction energies determined by extended Hückel calculations amount to 0.27 and 0.21 eV in the Mo and W salts, respectively. Furthermore, short intermolecular lateral contacts between dimers (S$\cdots$S 3.671(5) and S$\cdots$Se 3.634(4) Å in the Mo salt, and S$\cdots$S 3.673(5) and S$\cdots$Se 3.654(5) Å in the W salt) link the dimers with each other, thus giving rise to an alternated chain of [Cp$_2$M(dsit)$^{+\cdot}$] cations (Figure 12). The temperature dependence of the
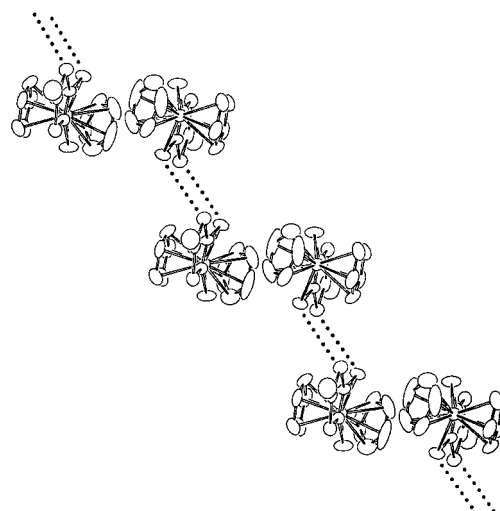

Figure 12. The chain structure of the [Cp$_2$M(dsit)]$^{+\cdot}$ cations (M = Mo, W). The dotted lines show the inter-dimer chalcogen–chalcogen interactions.

susceptibility of the two complexes is given in Figure 13. Data for the molybdenum salt are satisfactorily simulated within the antiferromagnetic uniform chain model[41, 42] for which an
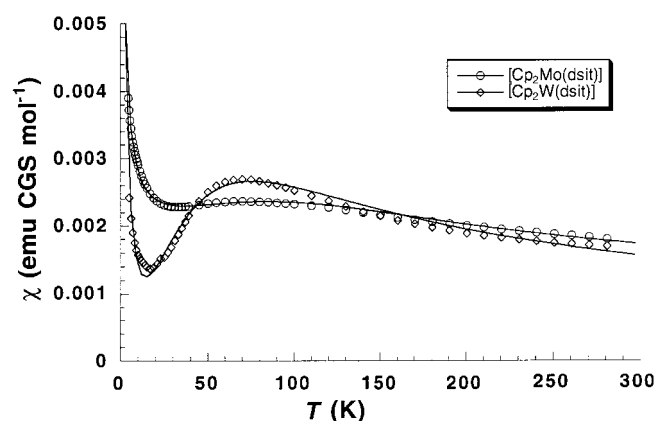

Figure 13. Temperature dependence of the magnetic susceptibility of [Cp$_2$Mo(dsit)][TCNQF$_4$] and [Cp$_2$W(dsit)][TCNQF$_4$]. The solid line is a fit to the alternated chain model (see text).

analytical expression has been derived [Eq. (4)],[43, 44] in which $x = |J|/kT$.

$$\chi_{mol} = \chi_0 + \frac{C_1}{T} + \frac{Ng^2\beta^2}{kT} \frac{0.25 + 0.07497x + 0.075235x^2}{1.0 + 0.9931x + 1.172135x^2 + 0.757825x^3} \quad (4)$$

We found $J_{Mo}/k = -147$ K, $C_1 = 0.010$ K^{-1} (i.e. 2.7% spin per mole) and $\chi_0 = 7.4 \times 10^{-4}$ emu mol^{-1}. For [Cp$_2$W(dsit)]-[TCNQF$_4$], the more pronounced susceptibility maximum reflects some higher degree of alternation in the cation chain. The best fit was obtained within the alternated chain model[45, 46] with $J_W/k = -113$ K and $\alpha = 0.5$. These large J values compare favorably with the EH calculated intra-dimer interaction energies mentioned above with $\beta_{Mo} = 0.27$ eV, $\beta_W = 0.21$ eV, and $(\beta_{Mo}/\beta_W)^2 = 1.6$, the latter can be compared with $J_{Mo}/J_W = 1.3$.

Conclusion

Three different structural patterns of association are identified and serve to demonstrate the potential of flexible organometallic complexes for the construction of electro-active materials. The dithiolene ligand modifications (O vs. S vs. Se), and the metal substitution (Mo vs. W) not only modify the geometrical characteristics of the individual molecules but also modulate the extent of delocalization of the radical species between the cyclopentadienyl, the metal, and the dithiolene moieties, and have a direct consequence on the possible intermolecular arrangements and their associated magnetic behavior. Furthermore, in the isostructural Mo and W salts (with dmid^{2-} and dsit^{2-}), the substitution of W for Mo only has a slight influence on the *molecular* structures but a considerable one on the *electronic* structures, as reflected by different spin gap values (Δ_{Mo}, Δ_W) in the [Cp$_2$M(dmid)] spin ladders or different alternation parameters (α_{Mo}, α_W) in the [Cp$_2$M(dsit)] alternated chains. This illustrates the extreme sensitivity of the solid-state electronic properties of molecular materials to minute changes of the molecular shapes and intermolecular interactions.

Experimental Section

[Cp$_2$Mo(dmit)] and [Cp$_2$Mo(dmid)] complexes were prepared as previously described from the reaction of [Cp$_2$MoCl$_2$] (Strem Chemicals) with the corresponding sodium salt of the desired dithiolene.[30] The corresponding [Cp$_2$W(dmit)] and [Cp$_2$W(dmit)] complexes were prepared analogously.[47] The precursor of the dsit^{2-} ligand, dsit(COPh)$_2$, was prepared according to the literature.[48]

[Cp$_2$Mo(dsit)]: To a solution of dsit(COPh)$_2$ (0.5 g, 1 mmol) in dry THF (50 mL) was added a solution of tBuCH$_2$ONa (1.45 M, 1.4 mL, 1 mmol) in toluene. After the mixture has been stirred for 1 h, solid [Cp$_2$MoCl$_2$] was added, and the solution warmed to reflux for 2 d. After evaporation of the cooled suspension, the residue was Soxhlet extracted with 1,1,2-trichloro-ethane, and the solution was filtered on a short silica gel column. Concentration afforded [Cp$_2$Mo(dsit)] as a violet microcrystalline powder (0.22 g, 43%). Elemental analysis calcd for C$_{13}$H$_{10}$MoS$_3$Se$_2$: C 30.24, H 1.95; found: C 29.68, H 1.96.

[Cp$_2$W(dsit)]: A solution of tBuCH$_2$ONa (1.45 M, 2.25 mL, 3.2 mmol) in toluene was added to a solution of dsit(COPh)$_2$ (400 mg, 0.8 mmol) in dry THF (50 mL). After stiring the solution for half an hour, [Cp$_2$WCl$_2$] (Strem Chemicals, 300 mg, 0.779 mmol) was added. The solution was refluxed for 36 h, and the product was then purified by chromatography on a silica gel column (CH$_2$Cl$_2$/cyclohexane, 4/1). The solution was concentrated and cooled to 4°C overnight. The crystalline precipitate was filtered and washed with cyclohexane (0.22 g, 45%). Elemental analysis calcd for C$_{13}$H$_{10}$S$_3$Se$_2$W$_1$: C 25.84, H 1.67, S 15.92; found: C 25.73, H 1.84, S 15.88.

Charge-tranfer salts with TCNQF$_4$: All salts were prepared by mixing hot solutions of TCNQF$_4$ dissolved in dry CH$_3$CN and the dithiolene complex dissolved in CH$_2$Cl$_2$ (for the Mo complexes) or in CH$_3$CN (for the W complexes). Slow cooling of the resulting dark solutions, which were then stored at 4–6°C overnight afforded black crystals of the title compounds.

[Cp$_2$Mo(dmid)][TCNQF$_4$]: Elemental analysis calcd for C$_{25}$H$_{10}$F$_4$Mo$_1$-N$_4$O$_1$S$_4$: C 43.99, H 1.48, N 8.21, S 18.79; found: C 41.68, H 1.71, N 8.24, S 18.51%.

[Cp$_2$W(dmid)][TCNQF$_4$]: Elemental analysis calcd for C$_{25}$H$_{10}$F$_4$N$_4$O$_1$S$_4$W$_1$: C 38.97, H 1.31, N 7.27, S 16.65; found: C 38.67, H 1.68, N 7.18, S 16.63%.

[Cp$_2$Mo(dsit)][TCNQF$_4$]: Elemental analysis calcd for C$_{25}$H$_{10}$F$_4$Mo$_1$N$_4$S$_3$Se$_2$: C 37.89, H 1.27, N 7.07, S 12.14; found: C 35.86, H 1.76, N 5.81, S 13.82%.

[Cp$_2$W(dsit)][TCNQF$_4$]: Elemental analysis calcd for C$_{25}$H$_{10}$F$_4$N$_4$S$_3$Se$_2$W$_1$: C 34.11, H 1.14, N 6.36, S 10.93; found: C 33.88, H 1.25, N 6.30, S 10.05%.

[Cp$_2$Mo(dmit)]$_2$[TCNQF$_4$]: Mixing solutions of [Cp$_2$Mo(dmit)] and TCNQF$_4$ led to the rapid precipitation of thin needlelike crystals which analyses as a 2:1 phase, [Cp$_2$Mo(dmit)]$_2$[TCNQF$_4$]. Elemental analysis calcd for C$_{38}$H$_{20}$F$_4$Mo$_2$N$_4$S$_{10}$: C 40.71, H 1.80, N 5.00, S 28.60; found: C 40.51, H 2.06, N 4.86, S 27.79%. Only a few crystals were suitable for X-ray structural analysis and crystal structure resolution shows them to be a solvated 1:1 phase, [Cp$_2$Mo(dmit)][TCNQF$_4$](CH$_2$Cl$_2$)$_{0.33}$. Attempts to modify the stoichiometry of the major phase by changing the ratio of the two components or the solvents used were unsuccessful.

[Cp$_2$W(dmit)][TCNQF$_4$]: Elemental analysis calcd for C$_{25}$H$_{10}$F$_4$N$_4$S$_5$W$_1$: C 38.18, H 1.28, F 9.66, N 7.12, S 20.38; found: C 38.14, H 1.47, F 8.93, N 7.29, S 20.39%.

X-Ray diffraction studies: Crystallographic data are given in Table 6. Data for [Cp$_2$Mo(dmid)][TCNQF$_4$] and [Cp$_2$Mo(dsit)][TCNQF$_4$] were colleted on a Enraf-Nonius CAD4-F diffractometer, the structures were solved by direct methods and refined against F using the Xtal 3.4 set of programs.[49] Data for the four other salts were collected on a Stoe Imaging Plate Diffractometer (IPDS), the structures were solved by direct methods and refined against F^2 using the SHELXTL5.04 set of programs.[50] Hydrogen atoms were placed at calculated positions (C–H = 0.93 Å), included in structure factor calculations but not refined (riding model). In the structure of [Cp$_2$Mo(dmit)][TCNQF$_4$][CH$_2$Cl$_2$]$_{0.33}$, one of the cyclopentadienyl rings was found to be disordered at two positions, with a 50:50 occupation. Furthermore, a disordered dichloromethane molecule was identified near an inversion center; the chlorine atoms common to the two molecules are related by the inversion center. Refinement of the occupation parameter s of carbon and chlorine atoms converges to 0.31 and 0.68, respectively, and was then set to 0.33 for a given CH$_2$Cl$_2$ molecule.

Table 6. Crystallographic data.

	Mo/dmid	W/dmid	Mo/dmit	W/dmit	Mo/dsit	W/dsit
chem. form.	$C_{13}H_{10}MoOS_4$, $C_{12}F_4N_4$	$C_{13}H_{10}OS_4W$, $C_{12}F_4N_4$	$C_{13}H_{10}MoS_5$, $C_{12}F_4N_4$, $(CH_2Cl_2)_{0.33}$	$C_{13}H_{10}S_5W$, $C_{12}F_4N_4$	$C_{13}H_{10}MoSe_2S_3$, $C_{12}N_4F_4$	$C_{13}H_{10}WS_3Se_2$, $C_{12}F_4N_4$
fw	682.58	770.46	726.95	786.52	792.43	880.32
temperature [K]	293	293	293	293	293	293
space group	$P\bar{1}$	$P\bar{1}$	$P\bar{1}$	$P\bar{1}$	$P2_1/c$	$P2_1/c$
a [Å]	13.041(2)	13.064(3)	6.638(1)	7.6593(10)	9.748(1)	9.7666(5)
b [Å]	14.381(2)	14.349(3)	11.685(1)	12.558(2)	14.354(1)	14.376(1)
c [Å]	7.327(4)	7.388(1)	18.780(2)	14.184(2)	18.535(3)	18.5379(7)
α [°]	98.77(3)	98.80(3)	107.34(1)	98.340(14)	–	–
β [°]	103.47(2)	103.39(3)	91.14(1)	101.816(14)	97.905(14)	97.970(5)
γ [°]	108.31(1)	108.38(3)	98.50(1)	103.865(14)	–	–
V [Å³]	1230.2(8)	1239.6(4)	1372.0(3)	1269.2(3)	2568.8(6)	2577.7(2)
Z	2	2	2	2	4	4
ρ_{calcd} [g cm⁻³]	1.843	2.064	1.759	2.058	2.049	2.268
μ [mm⁻¹]	0.93	5.056	0.976	5.017	3.64	7.60
crystal size	$0.4 \times 0.16 \times 0.06$	$0.135 \times 0.065 \times 0.05$	$0.24 \times 0.06 \times 0.03$	$0.17 \times 0.08 \times 0.02$	$0.3 \times 0.3 \times 0.02$	$0.16 \times 0.03 \times 0.007$
diffract.	Enraf CAD4	Stoe IPDS	Stoe IPDS	Stoe IPDS	Enraf CAD4	Stoe IPDS
octants collected	$h, \pm k, \pm l$	$\pm h, \pm k, \pm l$	$\pm h, \pm k, \pm l$	$\pm h, \pm k, \pm l$	$h, k, \pm l$	$\pm h, \pm k, \pm l$
max h,k,l	17, 18, 9	14,16,8	7, 13, 21	8, 14, 16	12, 17, 22	11, 16, 20
θ range [°]	1.5 – 28	1.7 – 24.1	1.85 – 24	1.8 – 24	1.5 – 26	1.8 – 24
collection. method	ω-2θ	$\Delta\varphi = 1.7°$	$\Delta\varphi = 1.3°$	$\Delta\varphi = 1.8°$	ω-2θ	$\Delta\varphi = 1.3$
absorption. correction	ψ scan	numerical	semiempirical	numerical	ψ scan	numerical
T_{min}, T_{max}	0.598, 0.98	0.382,0.628	0.571,0.675	0.358, 0.79	0.830, 1.	0.214,0.806
data collected	6442	10385	10904	10563	5740	20835
unique data	5923	3684	4040	3753	5027	3893
R_{int}	0.012	0.042	0.25	0.032	0.020	0.153
programs	Xtal3.2	SHELXTL 5.04	SHELXTL 5.04	SHELXTL 5.04	Xtal3.2	SHELXTL 5.04
parameters refined	F	F^2	F^2	F^2	F	F^2
data for refinement	4456	3681	4040	3752	2331	3890
no of variables	352	352	342	352	352	352
$R(F)$	0.052	0.037	0.051	0.029	0.056	0.036
$R_w(F)$[b] or $R_w(F^2)$[c]	0.056[b]	0.091[c]	0.126[c]	0.078[c]	0.063[b]	0.069[c]
residual density [e Å³]	– 2.2, +1.8[d]	– 2.6, +1.6[d]	– 0.3, +0.4	– 1.4, +0.7	– 3.1, +1.9[a]	– 0.9, +0.5
goodness of fit	1.57	1.0	0.80	1.045	1.16	0.65

[a] $R(F) = \Sigma ||F_o| - |F_c|| / \Sigma |F_o|$. [b] $wR(F) = [\Sigma w (|F_o| - |F_c|)^2 / \Sigma w |F_o|^2]^{1/2}$. [c] $wR(F^2) = [\Sigma [w (F_o^2 - F_c^2)^2] / \Sigma [w (F_o^2)^2]]^{1/2}$. [d] Residual density was found near the Mo or W atom at a distance less than 1 Å.

Crystallographic data (excluding structure factors) for the structures reported in this paper have been deposited with the Cambridge Crystallographic Data Centre as supplementary publication no. CCDC-101010. Copies of the data can be obtained free of charge on application to CCDC, 12 Union Road, Cambridge, CB2 1EZ, UK (fax: (+44)1223-336-033; e-mail: deposit@ccdc.cam.ac.uk).

[1] a) J. C. McDonald, G. M. Whitesides, *Chem. Rev.* **1994**, *94*, 2383; b) M. Simard, D. Su, J. D. Wuest, *J. Am. Chem. Soc.* **1991**, *113*, 4696.

[2] O. Félix, M. W. Hosseini, A. De Cian, J. Fischer, *Angew. Chem.* **1997**, *109*, 83; *Angew. Chem. Int. Ed. Engl.* **1997**, *36*, 102.

[3] a) A. Dolbecq, M. Fourmigué, P. Batail, C. Coulon, *Chem. Mater.* **1994**, *6*, 1413; b) A. Dolbecq, M. Fourmigué, F. C. Krebs, P. Batail, E. Canadell, R. Clérac, C. Coulon, *Chem. Eur. J.* **1996**, *2*, 1275

[4] D. Jérome, H. J. Schultz, *Adv. Phys.* **1982**, *31*, 299.

[5] a) T. Ishiguro, K. Yamaji, *Organic Superconductors*, Springer, Berlin, **1990**; b) J. M. Williams, J. R. Ferraro, R. J. Thorn, K. D. Carlson, U. Geiser, H. H. Wang, A. M. Kini, M.-H. Whangbo, *Organic Superconductors (including Fullerenes)*, Prentice Hall, Englewood Cliffs, NJ, **1992**.

[6] *The Physics and Chemistry of Organic Superconductors* (Eds.: G. Saito, S. Kagoshima), Springer, Heidelberg, **1990**.

[7] C. P. Jr. Poole, H. A. Farach, R. J. Creswick, *Superconductivity*, Academic Press, San Diego, **1995**.

[8] *Extended Linear Chain Compounds*, Vol. 3 (Ed.: J. S. Miller), Plenum, New York, **1983**.

[9] a) O. Kahn, *Molecular Magnetism*, VCH, Weinheim, **1993**; b) R. L. Carlin, *Magnetochemistry*, chapter 7, Springer, Berlin, **1986**.

[10] H. Imai, T. Inabe, T. Otsuka, T. Okuno, K. Awaga, K. *Phys. Rev. B* **1996**, *54*, R6838.

[11] a) R.-M. Olk, B. Olk, W. Dietzsch, R. Kirmse, E. Hoyer, *Coord. Chem. Rev.* **1992**, *117*, 99; b) P. Cassoux, L. Valade, H. Kobayashi, A. Kobayashi, R. A. Clark, A. E. Underhill, *Coord. Chem. Rev.* **1991**, *110*, 115.

[12] a) E. Canadell, S. Ravy, J.-P. Pouget, L. Brossard, *Solid State Commun.* **1990**, *75*, 633; b) E. Canadell, I. E.-I. Rachidi, S. Ravy, J.-P. Pouget, L. Brossard, J.-P. Legros, *J. Phys. France* **1989**, *50*, 2967; c) M. Bousseau, L. Valade, J.-P. Legros, P. Cassoux, M. Garbauskas, L. V. Interrante, *J. Am. Chem. Soc.* **1986**, *108*, 1908; d) L. Brossard, M. Ribault, L. Valade, P. Cassoux, *Physica B & C (Amsterdam)* **1986**, *143*, 378; e) I. S. Jacobs, H. R. Jr. Hart, L. V. Interrante, J. W. Bray, J. S. Kasper, G. D. Watkins,

D. E. Prober, W. P. Wolf, J. C. Bonner, *Physica B (Amsterdam)* **1977**, *86 – 88*, 655.

[13] a) P. Batail, C. Livage, S. S. P. Parkin, C. Coulon, J. D. Martin, E. Canadell, *Angew. Chem.* **1991**, *103*, 1508; *Angew. Chem. Int. Ed. Engl.* **1991**, *30*, 1498; b) A. Pénicaud, P. Batail, P. Davidson, A.-M. Levelut, C. Coulon, C. Perrin, C., *Chem. Mater.* **1990**, *2*, 117.

[14] X. Yang, T. B. Rauchfuss, S. R. Wilson, *J. Am. Chem. Soc.* **1989**, *111*, 3465; b) F. Guyon, C. Lenoir, M. Fourmigué, J. Larsen, J. Amaudrut, *Bull. Soc. Chim. Fr.* **1994**, *131*, 217; c) S. Zeltner, W. Dietzsch, R.-M. Olk, R. Kirmse, R. Richter, U. Schroder, B. Olk, E. Hoyer, *Z. Anorg. Allg. Chem.* **1994**, *620*, 1768; d) S. Zeltner, R.-M. Olk, M. Pink, S. Jelonek, P. Jörchel, T. Gelbrich, J. Sieler, R. Kirmse, *Z. Anorg. Allg. Chem.* **1996**, *622*, 1979.

[15] a) F. Guyon, J. Amaudrut, M.-F. Mercier, K. Shimizu, *J. Organomet. Chem.* **1994**, *465*, 187; b) F. Guyon, M. Fourmigué, R. Clérac, J. Amaudrut, *J. Chem. Soc. Dalton Trans.* **1996**, 4093.

[16] I. V. Jourdain, M. Fourmigué, F. Guyon, J. Amaudrut, *J. Chem. Soc. Dalton Trans.* **1998**, 483.

[17] M. L. H. Green, W. B. Heuer, G. C. Saunders, *J. Chem. Soc. Dalton Trans.* **1990**, 3789.

[18] M. Fourmigué, C. Lenoir, C. Coulon, F. Guyon, J. Amaudrut, *Inorg. Chem.* **1995**, *34*, 4979.

[19] M. Fourmigué, C. Coulon, *Adv. Mater.* **1994**, *6*, 948.

[20] a) R.-M. Olk, W. Dietzsch, K. Köhler, R. Kirmse, J. Reinhold, E. Hoyer, L. Golic, B. Olk, *Z. Anorg. Allg. Chem.* **1988**, *567*, 131; b) S. Ikegawa, T. Nogami, Y. Shirota, *Bull. Chem. Soc. Jpn.* **1990**, *63*, 262

[21] a) R. Vicente, J. Ribas, C. Faulman, J.-P. Legros, P. Cassoux, P. *C. R. Acad. Sci. Ser. B* **1987**, *305*, 1055; b) R. Vicente, J. Ribas, C. Zanchini, D. Gatteshi, J.-P. Legros, C. Faulman, P. Cassoux, *Z. Naturforsch. B* **1988**, *43*, 1137; c) R. Vicente, J. Ribas, S. Alvarez, A. Segui, X. Solans, M. Verdaguer, *Inorg. Chem.* **1987**, *26*, 4004.

[22] R.-M. Olk, A. Röhr, J. Sieler, K. Köhler, R. Kirmse, W. Dietzsch, E. Hoyer, B. Olk, *Z. Anorg. Allg. Chem.* **1989**, *577*, 206.

[23] R. C. Wheland, E. L. Martin, *J. Org. Chem.* **1975**, *40*, 3101.

[24] R. C. Wheland, J. L. Gillson, *J. Am. Chem. Soc.* **1976**, *98*, 3916.

[25] D. A. Dixon, J. C. Calabrese, J. S. Miller, *J. Phys. Chem.* **1989**, *93*, 2284.

[26] For example, in $[Mo(dmit)_3]^{2-}$ and $[W(dmit)_3]^{2-}$ $d_{mean}(Mo-S) = 2.404$ Å and $d_{mean}(W-S) = 2.394$ Å (G. Matsubayashi, K. Douki, H. Tamura, M. Nakano, *Inorg. Chem.* **1993**, *32*, 5990) and similarly, in $[Mo(mnt)_3]^{2-}$ and $[W(mnt)_3]^{2-}$, $d_{mean}(Mo-S) = 2.373$ Å and $d_{mean}(W-S) = 2.371$ Å (G. F. Brown, E. I. Stiefel, *Inorg. Chem.* **1973**, *12*, 2140).

[27] J. W. Lauher, R. Hoffmann, *J. Am. Chem. Soc.* **1976**, *98*, 1729.

[28] D. Braga, F. Grepioni, *Chem. Commun.* **1996**, 571.

[29] E. Dagotto, T. M. Rice, *Science* **1996**, *271*, 618.

[30] Z. Hiroi, *J. Solid State Chem.* **1991**, *95*, 230.

[31] T. M. Rice, S. Gopalan, M. Sigrist, *Europhys. Lett.* **1994**, *23*, 445.

[32] T. Barnes, J. Riera, *Phys. Rev. B* **1994**, *50*, 6817.

[33] B. Chiari, O. Piovesana, T. Tarantelli, P. F. Zanazzi, *Inorg. Chem.* **1990**, *29*, 1172.

[34] H. Imai, T. Inabe, T. Otsuka, T. Okuno, K. Awaga, *Phys. Rev. B* **1996**, *54*, R6838.

[35] C. Rovira, J. Venciana, E. Ribera, J. Tarres, E. Canadell, R. Rousseau, M. Mas, E. Molins, M. Almeida, R. T. Henriques, J. Morgado, J.-P. Schoeffel, J.-P. Pouget, *Angew. Chem.* **1997**, *109*, 2417; *Angew. Chem. Int. Ed. Engl.* **1997**, *36*, 2324.

[36] T. Komatsu, N. Kojima, G. Saito, *Solid State Commun.* **1997**, *103*, 519.

[37] E. Dagotto, R. Riera, D. J. Scalapino, *Phys. Rev. B* **1992**, *45*, 5744.

[38] M. Troyer, H. Tsunetsugu, D. Würtz, *Phys. Rev. B*, **1994**, *50*, 13515.

[39] P. Pincus, *Solid State Commun.* **1972**, *11*, 305.

[40] See ref. [9a], chapter 8.

[41] J. C. Bonner, M. E. Fisher, *Phys. Rev. A.* **1964**, *135*, 640.

[42] W. E. Hatfield, *J. Appl. Phys.* **1981**, *52*, 1985.

[43] J. W. Hall; W. E. Marsh, R. R. Weller, W. E. Hatfield, *Inorg. Chem.* **1981**, *20*, 1033.

[44] The spin Hamiltonian used here is given in Equation (5).

$$\mathscr{H} = -J\sum_{i=1}^{n-1} \boldsymbol{S}_{A_i} \cdot \boldsymbol{S}_{A_{i+1}} \tag{5}$$

[45] a) J. W. Hall, W. E. Marsh, R. R. Weller, W. E. Hatfield, *Inorg. Chem.* **1990**, *20*, 1033; b) ref. [9a], chapter 11.

[46] The definition of J stems from the spin Hamiltonian in zero field given in Equation (6).

$$\mathscr{H} = -J\sum_{i=1}^{n/2} [\ \boldsymbol{S}_{A_{2i}} \boldsymbol{S}_{A_{2i-1}} + \alpha \boldsymbol{S}_{A_{2i}} \boldsymbol{S}_{A_{2i+1}}] \tag{6}$$

[47] I. V. Jourdain, unpublished results.

[48] a) R. M. Olk, A. R hr, B. Olk, E. Hoyer, *Z. Chem.* **1988**, *28*, 304; b) P. J. Nigrey, *Synth. Metals* **1988**, *27B*, 365.

[49] *Xtal3.4 User's Manual* (Eds.: S. R. Hall, G. S. D. King, J. M. Stewart), University of Western Australia: Lamb, Perth, **1995**.

[50] G. M. Sheldrick, SHELXTL, version 5.04, Siemens Analytical X-Ray Instruments, Madison, Wisconsin, USA.

[51] R. Hoffmann, *J. Chem. Phys.* **1963**, *39*, 1397.

[52] a) M.-H. Whangbo, J. M. Williams, P. C. W. Leung, M. A. Beno, T. J. Emge, H. H. Wang, K. D. Carlson, G. W. Crabtree, *J. Am. Chem. Soc.* **1985**, *105*, 5815; b) E. Clementi, C. Roetti, *At. Nucl. Data Tables*, **1974**, *14*, 177.